Roles of the Ubiquitin/Proteasome Pathway in Pollen Tube Growth with Emphasis on MG132-Induced Alterations in Ultrastructure, Cytoskeleton, and Cell Wall Components[1][W]

Xianyong Sheng, Zhenghai Hu, Hongfei Lü, Xiaohua Wang, František Baluška, Jozef Šamaj, and Jinxing Lin*

Institute of Botany, Chinese Academy of Sciences, Key Laboratory of Photosynthesis and Molecular Environment Physiology, Beijing 100093, China (X.S., H.L., X.W., J.L.); College of Life Science, Northwest University, Xi'an 710069, China (X.S., Z.H.); Institute of Cellular and Molecular Botany, Rheinische Friedrich-Wilhelms-University Bonn, Department of Plant Cell Biology, D–53115 Bonn, Germany (F.B., J.Š.); Institute of Botany, Slovak Academy of Sciences, SK–84223, Bratislava, Slovak Republic (F.B.); and Institute of Plant Genetics and Biotechnology, Slovak Academy of Sciences, SK–95007, Nitra, Slovak Republic (J.Š.)

The ubiquitin/proteasome pathway represents one of the most important proteolytic systems in eukaryotes and has been proposed as being involved in pollen tube growth, but the mechanism of this involvement is still unclear. Here, we report that proteasome inhibitors MG132 and epoxomicin significantly prevented *Picea wilsonii* pollen tube development and markedly altered tube morphology in a dose- and time-dependent manner, while hardly similar effects were detected when cysteine-protease inhibitor E-64 was used. Fluorogenic kinetic assays using fluorogenic substrate sLLVY-AMC confirmed MG132-induced inhibition of proteasome activity. The inhibitor-induced accumulation of ubiquitinated proteins (UbPs) was also observed using immunoblotting. Transmission electron microscopy revealed that MG132 induces endoplasmic reticulum (ER)-derived cytoplasmic vacuolization. Immunogold-labeling analysis demonstrated a significant accumulation of UbPs in degraded cytosol and dilated ER in MG132-treated pollen tubes. Fluorescence labeling with fluorescein isothiocyanate-phalloidin and β-tubulin antibody revealed that MG132 disrupts the organization of F-actin and microtubules and consequently affects cytoplasmic streaming in pollen tubes. However, tip-focused Ca^{2+} gradient, albeit reduced, seemingly persists after MG132 treatment. Finally, fluorescence labeling with antipectin antibodies and calcofluor indicated that MG132 treatment induces a sharp decline in pectins and cellulose. This result was confirmed by Fourier transform infrared analysis, thus demonstrating for the first time the inhibitor-induced weakening of tube walls. Taken together, these findings suggest that MG132 treatment promotes the accumulation of UbPs in pollen tubes, which induces ER-derived cytoplasmic vacuolization and depolymerization of cytoskeleton and consequently strongly affects the deposition of cell wall components, providing a mechanistic framework for the functions of proteasome in the tip growth of pollen tubes.

Most cellular proteins are continuously synthesized and degraded within the lifespan of a cell. Efficient protein turnover is essential for many aspects of cell physiology and development (Hellmann and Estelle, 2002). As one of the most important proteolytic pathways in eukaryotic cells, the ubiquitin/proteasome pathway (UPP) is believed to be involved in the degradation of the bulk of intracellular proteins, including misfolded proteins and short- and long-lived regulatory proteins (Glickman and Ciechanover, 2002; Ciechanover, 2005; Hershko, 2005; Varshavsky, 2005). Therefore, the biological functions of the UPP in both animal and plant systems have received considerable attention.

Pollen tubes are responsible for delivering sperm cells to the egg for fertilization and are therefore essential for higher plant sexual reproduction. The emergence and elongation of pollen tubes is a complex and intriguing example of cell morphogenesis. The control of this type of growth requires a number of factors and activities to be integrated in space and time (Mascarenhas, 1993; Taylor and Hepler, 1997; Moscatelli and Cresti, 2001). Previous reports have indicated that the UPP is involved in pollen germination and tube growth, and that inhibition of proteasome activity significantly decreases pollen tube growth and alters

[1] This work was supported by the National Science Fund of China for Distinguished Young Scholars (grant nos. 30225005 and 30570100), by the Deutsche Forschungsgemeinschaft (grant no. SA 1564/2–1 to J.Š.), by the European Union Research Training Network TIPNET (project HPRN–CT–2002–00265), by Grant Agency APVT (grant no. APVT–51–002302), by the Deutsches Zentrum für Luft- und Raumfahrt, and by the National Natural Science Foundation of China (grant no. 30370088).

* Corresponding author; e-mail linjx@ibcas.ac.cn; fax 0086–10–62590833.

The author responsible for distribution of materials integral to the findings presented in this article in accordance with the policy described in the Instructions for Authors (www.plantphysiol.org) is: Jinxing Lin (linjx@ibcas.ac.cn).

[W] The online version of this article contains Web-only data.

Article, publication date, and citation information can be found at www.plantphysiol.org/cgi/doi/10.1104/pp.106.081703.

pollen tube morphology in *Actinidia deliciosa* (Speranza et al., 2001; Scoccianti et al., 2003). Similar results were obtained in our preliminary study on the effects of MG132, a specific proteasome inhibitor, on *Picea wilsonii* pollen germination and tube growth (Sheng and Hu, 2005). However, the data available at present appear insufficient to provide complete knowledge of the functions of the UPP during pollen tube development. Particularly, no attention has been paid to the possible roles of the UPP in cytoskeleton organization, the polarized distribution of organelles, and the deposition of cell wall components, all of which are closely linked to tip growth in pollen tubes (Li et al., 1997; Taylor and Hepler, 1997; Parre and Geitmann, 2005).

To extend our knowledge of the involvement of the UPP in pollen tube growth, we provide here several lines of evidence about effects of the peptide aldehyde proteasome inhibitor MG132 on *P. wilsonii* pollen tube growth, including the germination, tube elongation, tip morphology, in vitro proteasome activity, and the level of ubiquitinated proteins (UbPs). Moreover, we present data on the inhibitor-induced alterations in the ultrastructure, the cytoskeleton, and the cell wall organization, providing further insights into the mechanism by which proteasome controls pollen tube growth.

RESULTS

Proteasome Inhibitors Prevent Pollen Tube Growth and Induce Morphological Changes

The germination of *P. wilsonii* pollen in standard germination medium is characterized by a long lag phase (about 12–16 h), after which the tube emerges and elongates. MG132 significantly delayed *P. wilsonii* pollen germination in a dose-dependent manner. Microscopic evaluation of pollen germination revealed that only 54.04%, 43.3%, 29.35%, and 18.56% of pollen grains germinated when treated with 10, 20, 40, or 80 μM MG132 for 20 h, respectively, whereas at this time, about 62.9% of untreated pollen grains had germinated. Although the germination rate of inhibitor-treated pollen grains increased over time, there was a marked difference between the germination rates of control and MG132-treated pollen grains, especially at concentrations of MG132 between 20 and 80 μM. In addition, MG132 consistently reduced pollen tube elongation in a dose- and time-dependent manner. As shown in Figure 1A, pollen tubes cultured under control conditions grew at an average rate of 10.11 μm h^{-1}, whereas the growth rates of pollen tubes treated with various concentrations of MG132 were only 9.05 (10 μM), 7.08 (20 μM), 5.39 (40 μM), or 4.42 μm h^{-1} (80 μM), respectively. As a result, after 32 h of incubation, the average lengths of MG132-treated tubes were 198.49 μm (10 μM), 157.57 μm (20 μM), 125.23 (40 μM), or 108.73 μm (80 μM), as compared to the 223.83 μm of control tubes.

The morphology of pollen tubes was also strongly affected by MG132 treatment. Under control conditions, *P. wilsonii* pollen tubes are elongated with a uniform diameter. Amyloplasts are observed throughout the tube except in the elongating tip (Fig. 2A). The typical morphological organization of pollen tubes was strongly affected by MG132, particularly in the apical and subapical regions. The most obvious phenomenon was strongly cytoplasmic vacuolization, which was not observed in control tubes. Statistical analysis indicated that more than 50% of the emerging tubes was extensively vacuolated following treatment with 20 μM MG132 for 24 h, while the data reached 85% when treated with 40 μM MG132 for the same time. Monitoring the development of MG132-induced vacuolization by microscopy revealed that, initially, a

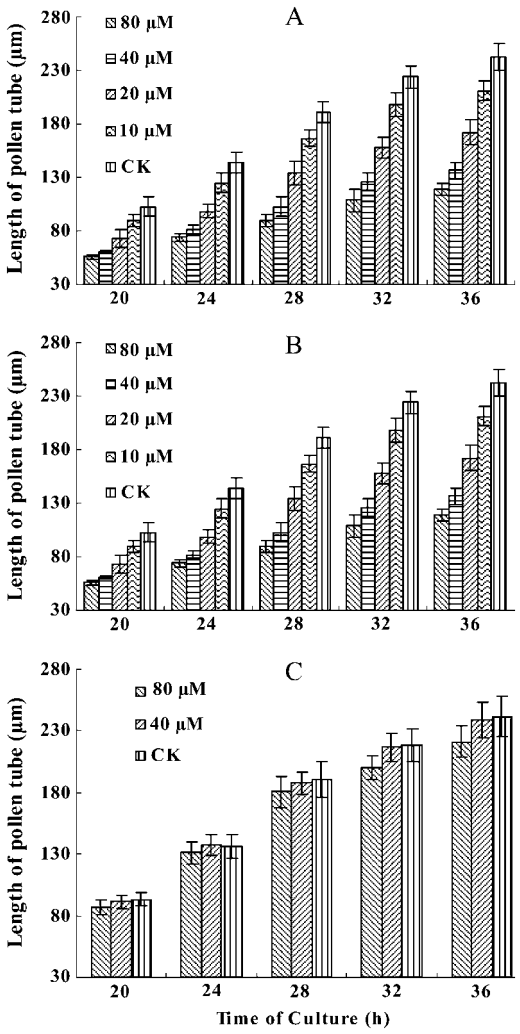

Figure 1. Effects of MG132, epoxomicin, and E-64 on *P. wilsonii* pollen tube growth. A, Effects of MG132 on pollen tube growth. CK, 10, 20, 40, and 80 μM represent pollen grains/tubes treated with 0, 10, 20, 40, or 80 μM MG132, respectively. B, Effects of epoxomicin on pollen tube growth. CK, 1, 2, and 4 μM represent pollen grains/tubes treated with 0, 1, 2, or 4 μM epoxomicin, respectively. C, Effects of E-64 on pollen tube growth. CK, 40 and 80 μM represent pollen grains/tubes treated with 0, 40, or 80 μM E-64, respectively. All data represent means ± SD of three independent experiments.

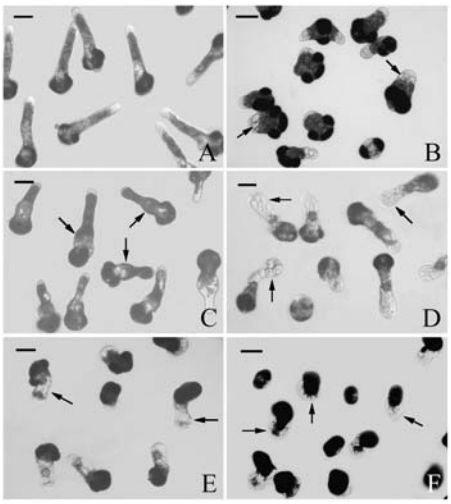

Figure 2. Effects of MG132 on *P. wilsonii* tube morphology. A, Pollen tubes cultured under control conditions for 24 h, showing normal length and shape. B, Pollen tubes treated with 40 μM MG132 for 20 h, showing the formation of vacuoles at the subapical region of the tube (arrows). C, Pollen tubes treated with 40 μM MG132 for 20 h, then MG132 was washed out, and tubes were cultured in fresh medium without inhibitor for additional 8 h. Note that tubes could recover their growth with normal morphology except obviously broadened base of tubes from previous treatment. D, Pollen tubes treated with 40 μM MG132 for 24 h, showing the inhibitor-induced cellular vacuolization, tip swelling (arrows), and irregularly broadened diameter. E, Pollen tubes treated with 2 μM epoxomicin for 24 h, arrows indicate the inhibitor-induced cellular vacuolization, tip swelling, and irregularly broadened diameter. F, Pollen tubes treated with 4 μM epoxomicin for 24 h, arrows show the serious effects on tube morphology and severe growth inhibition. Bars = 50 μm.

few small vacuoles occurred in the subapical regions of inhibitor-treated tubes (Fig. 2B). With increasing time of treatment, the number of small vacuoles increased, and subsequently they coalesced into larger vacuoles, ultimately occupying nearly the whole tube (Fig. 2D). In addition, cytoplasmic vacuolization was frequently accompanied by swollen tips and irregular tube diameters (Fig. 2D). The diameter of MG132-treated tubes often varied drastically within the same tube. Similar phenomena were observed when pollen tubes were cultured under control conditions for 20 h and then treated with 40 μM MG132 for 4 to 8 h (data not shown). Moreover, when MG132 was removed after 20 h and tubes were allowed to recover in fresh medium for additional 8 h, the inhibitor-induced vacuoles gradually regressed and eventually disappeared. Most of the tubes developed morphology similar to that of control tubes, except broader tube bases caused by previous effects of MG132 (Fig. 2C).

Given that MG132 can inhibit calpains as well as proteasome (Lee and Goldberg, 1998) and its side effects in plants are virtually unknown, the effects of other inhibitors, epoxomicin as a more specific proteasome inhibitor and E-64 as a Cys-protease inhibitor, were also investigated in this study. The results indicated that epoxomicin treatment strongly inhibited *P. wilsonii* pollen germination in a dose-dependent manner. Only 49.37% of pollen grains germinated when pollen grains were treated with 1 μM epoxomicin for 20 h, and the data sharply reduced to 36.22% and 13.58% when concentrations of epoxomicin increased to 2 and 4 μM, respectively. Similarly to MG132 treatment, inhibition of proteasome via epoxomicin also significantly reduced pollen tube growth. As shown in Figure 1B, the corresponding growth rates of epoxomicin-treated pollen tubes were 5.81 (1 μM), 3.15 (2 μM), and 1.75 μm h^{-1} (4 μM). Besides, epoxomicin treatment significantly induced morphological changes including vacuolization and pollen tube swelling (Fig. 2, E and F), which were consistent with MG132 treatments. On the other hand, though E-64 treatment slightly inhibited pollen tube growth (this inhibition was, however, not statistically significant; see Fig. 1C), no significant changes were observed on pollen germination rate and tube morphology (data not shown).

MG132 Inhibits Proteasome Activity, Resulting in the Accumulation of UbPs in Pollen Tubes

To demonstrate that proteasome activity is required during pollen tube growth and that the significant changes induced by MG132 in pollen tubes are due to the inhibition of proteasome activity, the proteasome activities in crude pollen tube extracts containing various concentrations of MG132 were measured by monitoring the release of the fluorophore 7-amido-4-methylcoumarin (AMC) from the synthetic peptide suc-Leu-Leu-Val-Tyr (sLLVY)-AMC, a substrate for the chymotryptic-like activity of the proteasome (Lightcap et al., 2000). Crude extracts obtained from pollen tubes cultured for 24 h showed a high ability to hydrolyze the fluorogenic substrate in the absence of MG132. As shown in Figure 3, the fluorescence derived from AMC increased linearly over time at a rate of approximately 62.67 fluorimetric units mg $protein^{-1}$ min^{-1}. In contrast, the cleavage of sLLVY-AMC was sharply reduced to only 83.16%, 58.97%, or 24.81% that of the control when 10, 20, or 40 μM MG132 were added to the extracts, respectively. The magnitude of proteasome inhibition was not significantly higher in extracts containing 80 μM MG132 than in extracts containing 40 μM MG132.

Because most substrate proteins are first ubiquitinated and then rapidly degraded by the proteasome, inhibition of proteasome activity should result in the accumulation of UbPs in pollen tubes. To further validate the proteasome inhibition assay, the level of UbPs was examined using an antiubiquitin antibody. The proteins extracted from pollen tubes of different stages of elongation shared similar patterns, at least within the limits of SDS-PAGE and Coomassie staining techniques (Fig. 4A). Immunoblots revealed several protein bands with different molecular masses that were recognized by the ubiquitin antibody (Fig. 4B), similar to previous reports in pine (*Pinus* spp.) pollen grains (Kulikauskas et al., 1995). The UbPs were

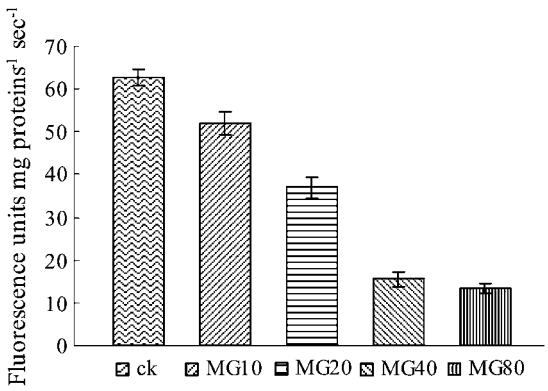

Figure 3. Proteasome activity measurement. Extracts of 24 h cultured pollen tubes were incubated in the presence of 120 μM sLLVY-AMC and various concentrations of MG132 at 24°C. The breakdown of the fluorogenic peptide was monitored by a fluorescence spectrophotometer for 5 min. MG10, MG20, MG40, and MG80 represent additions of 10, 20, 40, or 80 μM MG132, respectively, into extracts.

detectable after 6 h of incubation under control conditions, and their levels increased slightly over time. In contrast, treatment with 40 μM MG132 promoted the strong accumulation of UbPs in pollen tubes, demonstrating that the UbP bands were far more prevalent in MG132-treated tubes than in untreated tubes.

Since we focused in later experiments on the role of UPP in the cytoskeleton dynamics, it was necessary to understand whether actin and tubulin are substrates for the ubiquitin/proteasome complex, therefore western blots probed with antiactin or antitubulin antibodies were also performed. The results revealed that only one band was detected when antiactin (Fig. 4C) or anti-β-tubulin (data not shown) antibody was used, respectively, and that there was no significant difference in the intensity of actin and tubulin bands between control and MG132-treated pollen tubes when equal quantities of total pollen tube proteins were loaded on SDS-PAGE, similar to other reports (Speranza et al., 2001; Qiao et al., 2004). Since individual proteasome substrates are usually modified with varying numbers of ubiquitin molecules to produce a range of higher molecular mass proteins, the results presented here, together with other reports, demonstrated that neither actin nor tubulin was ubiquitinated.

MG132 Disrupts Polarized Distribution of Organelles and Induces Endoplasmic Reticulum-Derived Vacuolization in *P. wilsonii* Pollen Tubes

Transmission electron microscopy (TEM) revealed that the extreme apical zone of pollen tube was filled with numerous secretory vesicles (Fig. 5A). Fusion of vesicles with the plasma membrane was frequently observed, indicating that cell wall materials were actively released into the cell wall. The subapical zone was rich in all other organelles, especially in rough endoplasmic reticulum (rER; Fig. 5B). Much variation was observed in tubes treated with 40 μM MG132 for 20 h (Fig. 5, C–H). The most obvious change was a disruption of the polarized distribution of organelles, as shown by the sharp decline in the number of vesicles and the appearance of other organelles, including starch grains and vacuoles, at the apex of the tube (Fig. 5C). Fusion of vesicles with the apical plasma membrane was rarely observed, and the plasma membrane in this region was rather smooth. Furthermore, exposure of pollen tubes to MG132 induced dilatation of the rER and cytoplasmic vacuolization in a time-dependent manner (Fig. 5, D–H).

To confirm that the cellular vacuolization in the pollen tubes resulted from the inhibitor-induced accumulation of UbPs, immunogold labeling analysis was carried out using antiubiquitin antibody. In control tubes, gold particles were distributed randomly in the cytosol (Fig. 6A) and were sometimes near or in contact with the rER (Fig. 6B), but usually on the cytosolic face of the rER membrane. In contrast, the distribution and quantity of gold particles were markedly different in MG132-treated pollen tubes (Fig. 6, C–E; Fig. 7). In these tubes, gold particles were aggregated in degraded cytosol (Fig. 6C), on ER membranes, and even in the lumen of dilated ER (Fig. 6D). In addition, in treated tubes, both vegetative and generative nuclei were stained with far more gold particles than in control tubes, particularly at the chromatin (Fig. 6E).

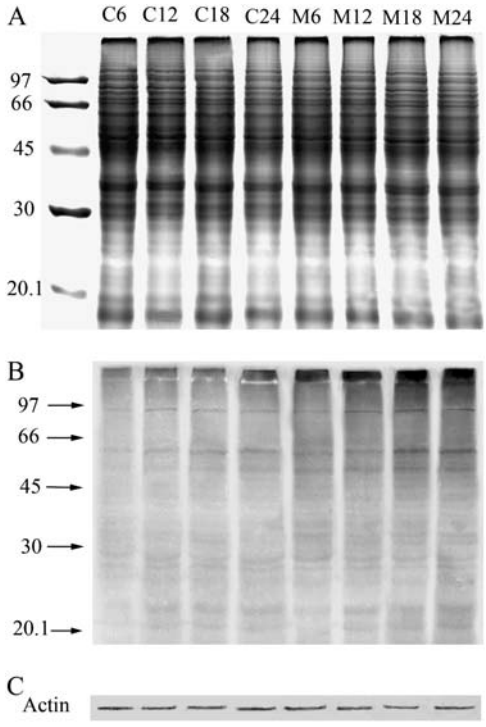

Figure 4. SDS-PAGE and immunoblotting analysis. Lanes M6, 12, 18, and 24 represent pollen grains/tubes treated with 40 μM MG132 for 6, 12, 18, and 24 h, respectively; lanes C6, 12, 18, and 24 represent pollen grains/tubes cultured under control conditions for 6, 12, 18, and 24 h, respectively. Molecular masses (in kilodaltons) of standard proteins are indicated on the left. A, Protein pattern obtained by SDS-PAGE and Coomassie Blue staining. B, Immunoblotting analysis with antiubiquitin antibody. C, Immunoblotting analysis with an antiactin antibody.

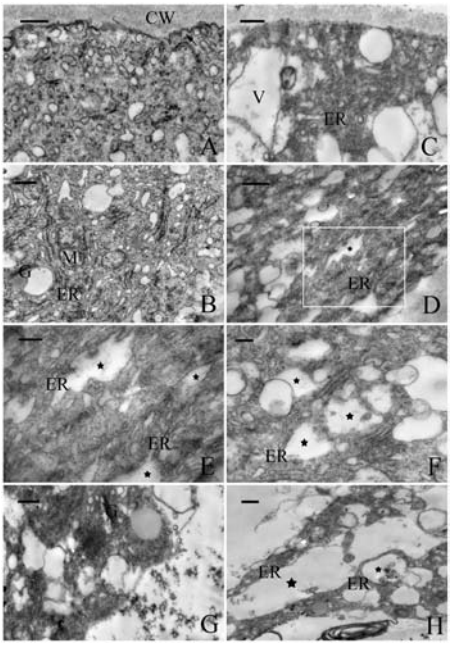

Figure 5. Electron micrographs of pollen tubes of *P. wilsonii* cultured in standard medium for 24 h (A and B) or treated with 40 μM MG132 for 20 h (C–G) or 24 h (H). A, The apical region of a control tube showing vesicle-rich zone. Note that some of these vesicles are fusing with the plasma membrane (indicated by arrow). B, The subapical region of a control tube, showing abundant organelles including ER, mitochondria (M), and Golgi stacks (G). C, The apical region of a treated pollen tube, showing dramatic decline in vesicles and appearance of vacuoles (V) and other organelles in this zone. D to H, The subapical region of treated tubes, showing MG132 induced ER dilatation (indicated by stars) and cellular vacuolization. Figure E represents magnified view of boxed area in Figure D (indicated by box). Bar = 0.5 μm for A to D and H and 0.2 μm for E to G.

Very few gold particles were visible in negative control sections prepared by omitting the primary antiubiquitin antibody (Fig. 6F). Data obtained using the point-counting method revealed significant differences between control and inhibitor-treated tubes. In particular, the mean densities of gold particles observed in the cytosol and ER of MG132-treated pollen tubes were 124% and 339% greater than in control tubes, respectively (Fig. 7).

MG132 Treatment Disrupts Cytoskeleton Organization and Cytoplasmic Streaming in Pollen Tubes

Because proteasomes have been observed in association with actin filaments (AFs) and actin-myosin complexes in animal cells (Arcangeletti et al., 1997, 2000), we hypothesized that inhibition of proteasome activity would disrupt the organization of AFs, which play a central role in the polarized tip growth of pollen tubes. To examine this possibility, the actin cytoskeleton in control and MG132-treated pollen tubes was compared using fluorescein isothiocyanate (FITC)-phalloidin staining. Confocal microscopic analysis revealed that in control tubes thick bundles of AFs were distributed throughout the length of the pollen tube in an axial array, except at the tip, where a dense array of fine AFs was frequently observed to extend into the diffusely staining apex (Fig. 8, A and B). On the other hand, in tubes treated with 40 μM MG132 for 20 h, the organization of AFs was markedly disturbed, showing a meshwork of short actin AFs extended into the extreme apex (Fig. 8, C and D). By 24 h, the short AFs had been further damaged, appearing as a diffuse staining pattern and small clumps of very short AFs (Fig. 8, E and F).

Given that MG132 has effects on the organization of the microtubule (MT) cytoskeleton in plant cells (Oka et al., 2004), it is necessary to investigate the effect of MG132 on MT organization in pollen tube, though the specific role of MTs in pollen tube is not clearly defined. In this study, immunolabeling with anti-β-tubulin antibody indicated that MTs are present throughout the pollen tube, forming a continuous network from the base to the apex of the pollen tube. In the shank of *P. wilsonii* pollen tubes, numerous long MTs show predominantly longitudinal orientation across each other and seemingly form a meshwork (Fig. 9A). However, MTs are enriched but distributed in a radial array at the apex of pollen tube (Fig. 9B). On the other hand, significant aberrations of MTs were observed in

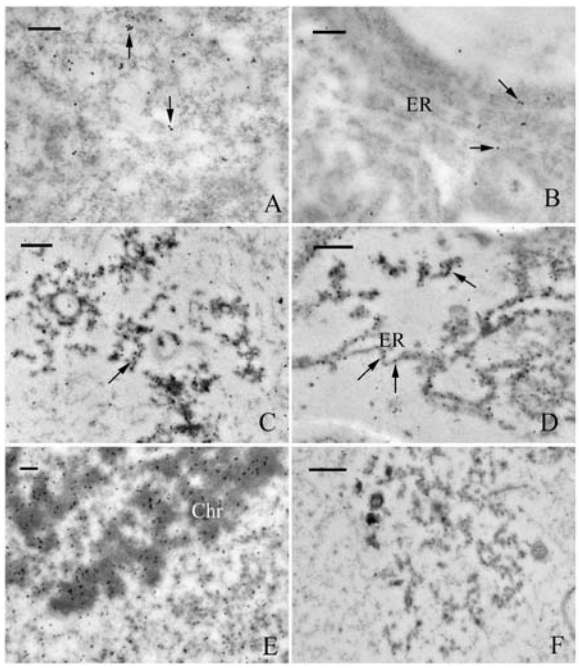

Figure 6. Immunogold labeling of UbPs. Pollen tubes cultured under control conditions (A and B) or treated with 40 μM MG132 (C–E) for 20 h. A, The cytosol with gold labeling on some vesicles and/or small vacuoles (arrows). B, Gold particles observed close to, or on the ER membranes (arrows). C, Gold particles deposited in the congregated and degraded cytosol (arrow). D, Numerous gold particles observed on the membrane and within the lumen of the dilated ER (arrows). E, Vegetative nucleus stained with many gold particles, particularly in the chromatin (chr). F, Few gold particles were visible in negative control. Bars = 0.2 μm.

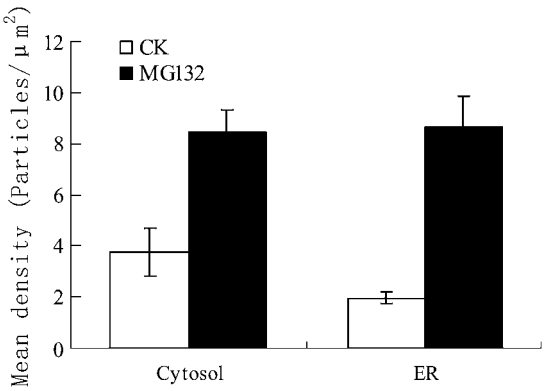

Figure 7. Quantification of UbPs immunogold labeling density. Histogram representing the number of gold particles per squared micrometer after immunogold labeling of UbPs in cytosol and ER of untreated tubes (white bars) and tubes treated with 40 μM MG132 for 20 h (black bars).

the tubes treated with 40 μM MG132 for 24 h. In the shank of inhibitor-treated tubes, MTs were fragmented, sinuous, and disorganized (Fig. 9C). Within the swollen tips, the radial array of cortical MTs is disrupted. Instead, MTs are very short and randomly distributed throughout the swollen tips (Fig. 9D).

Since calcium is another key regulator in tip growth of pollen tube, and the tip-focused Ca^{2+} gradient is also necessary for structural organization of cytoskeleton in angiosperm pollen tubes (Franklin-Tong, 1999), we further tested the possible effects of MG132 treatment on Ca^{2+} distribution. The results obtained using Fluo-3/AM staining indicated that a steep tip-to-base concentration gradient of cytosolic free Ca^{2+} was always observed in normally growing tube (Fig. 9E). This tip-focused Ca^{2+} gradient remained maintained in the swollen tip of MG132-treated tubes, though a far more rapid drop of the Ca^{2+} concentration was observed when compared with that in control tubes (Fig. 9F), suggesting that inhibitor treatment did not cause an apparent disruption of calcium gradient.

To further confirm the MG132-induced disruption of the cytoskeleton, confocal microscopy was used to visualize the cytoplasmic streaming in pollen tubes, a phenomenon that depends on intact cytoskeleton elements, especially actin microfilaments (Taylor and Hepler, 1997; Li et al., 2001; Justus, et al., 2004). As shown in Figure 10A (see also Supplemental Video 1), cytoplasm in control tubes streams in a fountain pattern or, rarely, in a reverse fountain pattern, similar to a previous report in *Picea abies* pollen tubes (Justus, et al., 2004). In contrast, the direction and speed of cytoplasmic streaming in MG132-treated tubes was markedly affected in a time-dependent manner. MG132 treatment for 20 h showed slight effect on the speed of cytoplasmic streaming, but the direction of cytoplasmic streaming changed markedly (data not shown). When tubes were treated with MG132 for 24 h, both the speed and the direction of cytoplasmic streaming were markedly affected (Supplemental Video 2). In a few strongly inhibited tubes, cytoplasmic streaming was almost completely stopped, and the motility of organelles was reduced to Brownian motion (Fig. 10B; Supplemental Video 3). On the other hand, recovery experiments indicated that after removing the MG132 from the growth medium, inhibitor-induced cytoplasmic vacuolization in subapex gradually disappeared. Synchronously, cytoplasm started to stream vigorously again (Fig. 10C; Supplemental Video 4). It is necessary to point out here that if pollen tubes were treated with MG132 for a longer time, such as 24 h, it was difficult for pollen tubes to recover cytoplasmic streaming to normal level.

MG132 Treatment Induces a Sharp Decline in the Major Pollen Tube Cell Wall Components

The cell wall is another key structural player that regulates pollen tube growth, given that plant cell expansion is believed to depend on an interplay between intracellular driving forces and the controlled yielding of the cell wall (Parre and Geitmann, 2005). Thus, we wondered whether MG132 treatment would disrupt the organization of the cell wall, resulting in tip swelling and irregularly broadened tube diameters. To examine this possibility, we studied the distribution of cell wall components in pollen tubes. The results of immunolabeling of pectins with JIM5 (anti-acidic pectin antibody) and JIM7 (antiesterified pectin antibody) are presented in Figure 11, A to D. The fluorescence signal revealed that in control tubes, acidic pectins were deposited along the tube, except in the apical region, where the signal was too faint to

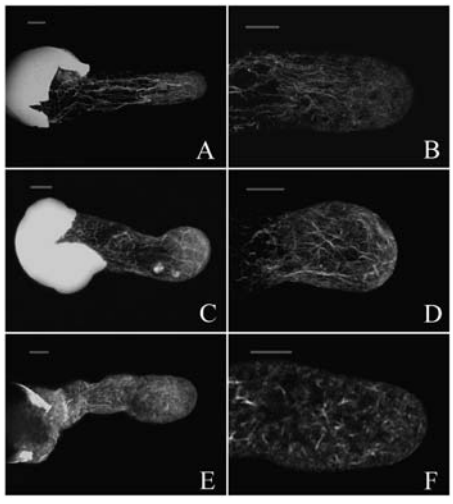

Figure 8. MG132-induced depolymerization of F-actin in pollen tubes. Samples were chemically fixed and stained with FITC-phalloidin. All tubes were visualized by confocal microscopy; the images were maximal projections of 30 to 50 optical sections at 0.5- or 1-μm intervals in the *z* axis. A and B, Control tubes cultured for 20 h. C and D, Tubes treated with 40 μM MG132 for 20 h. Note reorganization and fragmentation of AFs. E and F, Tubes treated with 40 μM MG132 for 24 h. Note severe fragmentation and disruption of AFs. Bar = 20 μm.

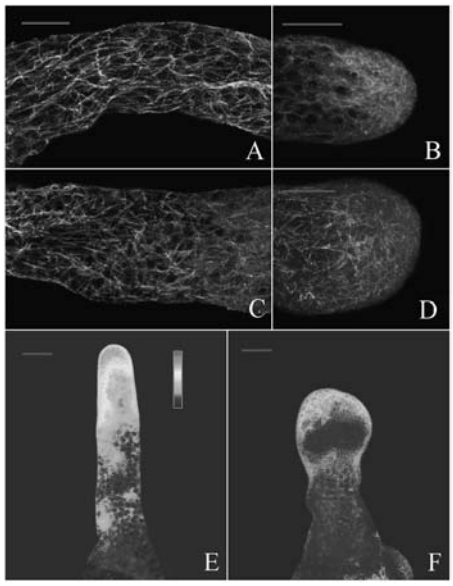

Figure 9. Effects of MG132 on MTs and cytosolic Ca^{2+} gradient. A to D, Samples were chemically fixed and immunolabeled with anti-β-tubulin antibody. E to F, Samples cultured with 40 μM MG132 for 24 h and incubated with Fluo-3/AM. All samples were visualized by confocal microscopy. A and B, Control tubes cultured for 24 h. C and D, Tubes treated with 40 μM MG132 for 24 h. Note reorganization and partial disruption of MTs. E, Distribution of cytosolic Ca^{2+} in the control tube. F, Distribution of cytosolic Ca^{2+} in the MG132-treated tube. Bar = 20 μm.

be detected (Fig. 11A). The bulk of esterified pectins were focused at the growing tip, with the intensity of the fluorescence signal decreasing gradually toward the base of the tube (Fig. 11C). In contrast, when tubes were treated with MG132, the distribution of pectin was significantly altered. The amount of acidic pectin was markedly decreased in MG132-treated tubes, especially in the subapical region (Fig. 11B). At the same time, the amount of esterified pectins at the tips of treated pollen tubes was dramatically lower than in control tubes, and they were evenly distributed (Fig. 11D). Calcofluor labeling revealed that cellulose was present throughout the control tubes, including the extreme tip, although the cellulose concentration was significantly lower at the apex than at the subapical region (Fig. 11E). On the other hand, a significant decline in cellulose was observed in the walls of MG132-treated tubes, especially at the subapical region (Fig. 11F). In severely inhibited tubes, little cellulose was detected in severely inhibited tubes, except at the base of the tubes (Fig. 11G). Interestingly, when tubes were cultured in standard medium for 20 h and then treated with MG132 for additional 8 h, almost no fluorescence derived from cellulose was detected in the extremely swollen tips, but the fluorescence was strong in other regions of the tube (Fig. 11H).

Using Fourier transform infrared (FTIR), we had mentioned in our preliminary report that MG132 treatment markedly reduced the content of wall-bound proteins and pectin in the apical regions of tubes (Sheng and Hu, 2005). To confirm the inhibitor-induced decline of cell wall components in pollen tubes, we further analyzed FTIR spectra obtained from apical regions, subapical regions, and basal regions of untreated tubes and MG132-treated tubes (Fig. 12). In a typical FTIR spectrum, amide-stretching bands derived from proteins occurred at 1,651 cm^{-1} (amide I) and 1,546 cm^{-1} (amide II), saturated esters absorbed at 1,740 cm^{-1} (McCann et al., 1994; Hao et al., 2005), and carboxylic acids absorbed at 1,414 cm^{-1} (McCann et al., 1992, 1994; Wang et al., 2005a). MG132-induced reductions in the main components of pollen tubes were observed in all three regions analyzed, but the components and the extent of these reductions varied within an individual tube. In the apices of pollen tubes, almost all components tested showed sharp declines, especially proteins and saturated esters. In the subapical region, the greatest reduction observed was in saturated esters and carboxylic acids. In the basal region, only amide II showed slight reduction, as compared to the levels in control tubes.

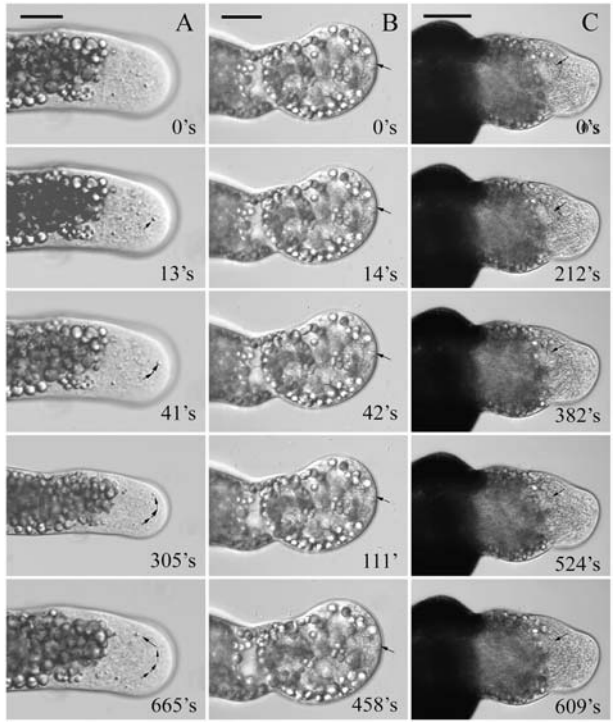

Figure 10. Effects of MG132 treatment on the cytoplasmic streaming. A, Control tube showing particles which moved quickly toward the tip in the tube center, and then moved away from the tip relatively slowly along the cell cortex (indicated by arrows; see also Supplemental Video 1). B, In the tube strongly inhibited by MG132, cytoplasmic streaming was almost completely stopped, especially in the apex and subapical region. (indicated by arrows; Supplemental Video 3). C, In the tubes treated with 40 μM MG132 for 20 h, and subsequently recovered in fresh culture medium for 1 h, vacuoles gradually disappeared from the tip (indicated by arrows) and accelerated cytoplasmic streaming was resumed (Supplemental Video 4). Bar = 20 μm.

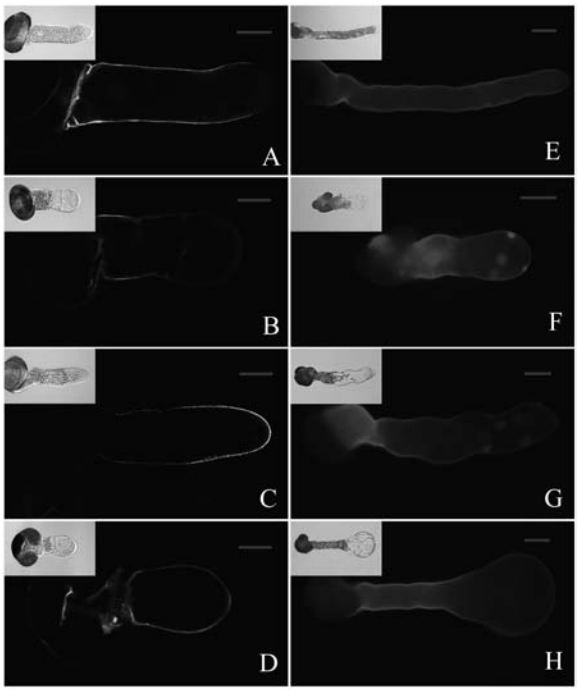

Figure 11. Effects of MG132 treatment on the distribution of pectin and cellulose in pollen tubes. A to D, Pollen tubes cultured for 24 h. Controls (A and C) and MG132-treated (B and D) were labeled either with JIM5 (A and B) or with JIM 7 (C and D) and visualized by confocal microscopy. E to H, Pollen tubes stained with calcofluor and visualized by fluorescent microscopy. E, Control tube cultured for 28 h. F, Pollen tube treated with 40 μM MG132 for 24 h. G, Pollen tube treated with 40 μM MG132 for 28 h. H, Pollen tube was cultured under standard control conditions for 20 h and then treated with MG132 for additional 8 h. Inserts represent corresponding differential interference contrast images. Bars = 20 μm for A to D and 40 μm for E to H.

DISCUSSION

MG132 is a reversible, membrane-permeable peptide aldehyde that inhibits the chymotrypsin-like activity of the proteasome. This compound is widely used as a proteasome inhibitor in both plant and animal systems (Lee and Goldberg, 1998). It has been reported that in vitro *A. deliciosa* pollen germination and tube growth are strongly affected by MG132 (Speranza et al., 2001). More recent studies have indicated that MG132 specifically blocks compatible pollination in Antirrhinum but has little effect on incompatible pollination, either in vitro or in vivo (Qiao et al., 2004). In our investigation, we found that MG132 not only significantly inhibited pollen tube emergence and elongation in a dose- and time-dependent manner (Fig. 1), but also induced significant morphological alterations including cytoplasmic vacuolization, swollen tips, and irregularly broadened tube diameters (Fig. 2). Nevertheless, MG132 may inhibit proteasome as well as calpains. Therefore, we tested epoxomicin as a potentially more specific inhibitor for the proteasome. Both MG132 and epoxomicin similarly inhibited pollen tube development and affected pollen tube morphology. On the other hand, these parameters were not affected by Cys-protease inhibitor E-64. Thus, our data are consistent and confirm previous reports that the strong effects in response to proteasome inhibitor MG132 were mainly due to the inhibition of proteasome (Speranza et al., 2001; Sheng and Hu, 2005).

Moreover, we found that in *P. wilsonii*, 20 to 40 μM MG132 caused moderate inhibition. This concentration is lower than that reported for angiosperms: 40 to 80 μM for *A. deliciosa* pollen tubes (Speranza et al., 2001) and 50 μM for Antirrhinum pollen tubes (Qiao et al., 2004). This difference in sensitivity to MG132 may account for the general differences in response to MG132 that have been observed in different plant species, because *P. wilsonii* pollen tubes grow far more slowly than angiosperm pollen tubes.

Degradation of proteins via the UPP involves two discrete and successive steps: (1) tagging of substrates by covalent attachment of ubiquitin, and (2) degradation of the tagged proteins by the proteasome complex with the release of free and reusable ubiquitin (Glickman and Ciechanover, 2002). The UPP exists in all eukaryotic cells tested, including angiosperm pollen tubes (Speranza et al., 2001; Qiao et al., 2004). Free ubiquitin and UbPs have also been reported to exist in pine pollen grains (Kulikauskas et al., 1995). In this study, both proteasome activity and several bands of UbPs were detected in *P. wilsonii* pollen tubes, indicating that the UPP is required in gymnosperms as well as in angiosperms. Although the functions of UbPs in *P. wilsonii* pollen tubes are still unclear, the several UbPs of different molecular masses detected in all samples by SDS-PAGE and western blotting suggest a broad diversity of proteasome substrates, implying a complex role for the UPP during pollen tube growth. Furthermore, an in vitro proteasome activity assay with

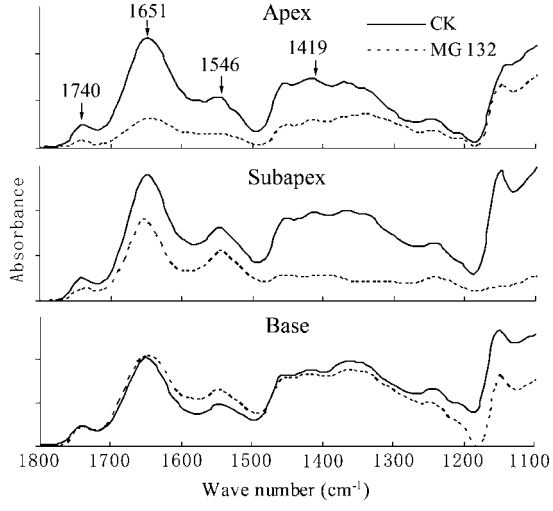

Figure 12. FTIR analysis. FTIR spectra were obtained from the tip, middle, and basal regions of pollen tubes cultured in standard medium (CK) or treated with 40 μM MG132 for 24 h. The data revealed that MG132 treatment induced significant decline of main cell wall components, especially at the apex and subapical region.

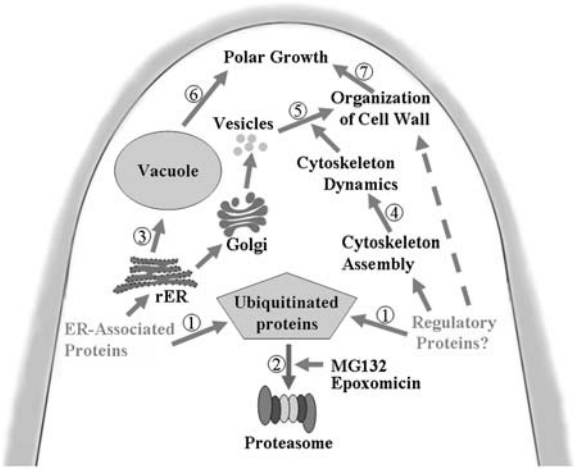

Figure 13. Hypothetical model summarizing effects of proteasome inhibitors on the tip growth of *P. wilsonii* pollen tubes. Part of ER-associated proteins and regulatory proteins essential for cytoskeleton assembly are ubiquitinated (1) and then degraded by 26S proteasome (2) during pollen tube growth. Inhibition of proteasome activity promotes accumulation of UbPs, which causes ER-derived vacuolization (3) and disruption of cytoskeleton (4) in pollen tubes. Consequently, reduction of vesicle trafficking (5) results in the disorganization of cell wall. Simultaneous vacuolization (6) and weakening of cell wall (7) lead to the disruption of tip growth, accompanied by irregularly broadened tube diameter and/or swollen tip.

various concentrations of MG132 caused the blocking of proteasome function in a dose-dependent manner (Fig. 3). These data correlated very well in accordance with the MG132-induced inhibition of pollen tube growth, as well as with morphological changes. In addition, immunoblotting revealed that the abundance and density of UbPs obtained from MG132-treated tubes were higher than those in control tubes (Fig. 4), which is similar to previous reports (Speranza et al., 2001; Scoccianti et al., 2003). This result was further supported by the results obtained from immunogold labeling analysis. All of these data enable us to conclude that the UPP is involved in pollen tube growth and that the inhibitor-induced accumulation of UbPs causes severe alterations in *P. wilsonii* pollen tubes.

Our new findings have revealed that MG132 induces cytosolic vacuolization in *P. wilsonii* pollen tubes in a dose- and time-dependent manner and that the inhibitor-induced vacuolization is reversible when MG132 is removed from the culture medium (Fig. 2C). Wagenknecht et al. (2000) reported that MG132 induces ER dilatation and cytoplasmic vacuolization in human malignant glioma cells. Similar cellular vacuolization in response to other proteasome inhibitors, such as PS-341, has also been observed in other tumor cells (Fribley et al., 2004; Mimnaugh et al., 2004). Our TEM analysis revealed abundant ER in control tubes, especially in the subapical region. In contrast, MG132 treatment induced ER dilatation and cytosolic vacuolization in a time-dependent manner (Fig. 5). These findings indicate that MG132 induces ER-derived cytosolic vacuolization in *P. wilsonii* pollen tubes.

The ER is an entrance compartment to the secretory pathway (Vitale and Denecke, 1999). The secretion of proteins is initiated by their uptake into the ER, where they are assembled and travel through the Golgi apparatus toward the cell surface. It is widely believed that the ER possesses a quality control mechanism now designated ERAD (ER-associated degradation), which ensures that only correctly folded, processed, and completely assembled proteins can exit this compartment for further transport through the secretory pathway (Vitale and Denecke, 1999; Hampton, 2002). There is increasing evidence that the UPP is involved in ERAD. Abnormal ER lumen proteins are believed to be transported out of the ER lumen to cytosol where they are ubiquitinated and subsequently degraded by cytosolic proteasomes (Hiller et al., 1996; Werner et al., 1996; Rabinovich et al., 2002). Our immunogold labeling with antiubiquitin antibody resulted in gold particles distributed randomly in the cytosol and sometimes close to or actually on the ER membranes in control tubes. This is similar to a previous report in olive (*Olea europaea*) pollen grains (Alché, et al., 2000), suggesting that the UPP is active in the degradation of denatured proteins. In contrast, far more gold particles were observed in MG132-treated pollen tubes, especially on the ER membranes (Fig. 6), providing direct proof of the MG132-induced accumulation of UbPs in the cytosol and ER. The toxic accumulation of these UbPs in pollen tubes might help to explain the ER dilatation and consequent cytosolic vacuolization that resulted from the inhibition of proteasome activity. The accumulation of gold particles in the ER, and especially on the ER membrane as observed in MG132-treated tubes, also confirmed that the UPP is involved in ERAD, whereas the ER membrane is the site at which misfolded or nonassembled lumen proteins are ubiquitinated (Hiller et al., 1996; Werner et al., 1996; Rabinovich et al., 2002). The rate of pollen tube growth depends on the efficient fusion of secretory vesicles with the plasma membrane to provide new plasma membrane and cell wall components necessary for the polar tip growth of pollen tubes (Mascarenhas, 1993; Li et al., 1997). The disorder inflicted on the secretory system by MG132 treatment, especially on the ER, would inevitably reduce the elongation of the tubes, as observed in our study.

It has long been appreciated that AFs control cytoplasmic streaming and hence the transport of secretory vesicles (Taylor and Hepler, 1997; Li et al., 2001; Justus et al., 2004). More recent evidence indicates that, in addition to actomyosin-driven streaming, actin polymerization itself also contributes to pollen tube growth, either as a force generator (Baluška and Volkmann, 2002) or as an organizer of the apical cytoplasm (Vidali and Hepler, 2001; Vidali et al., 2001). Besides, elongation of gymnosperm pollen tubes is believed to be dependent not only on F-actin and myosins but also on an intact MT cytoskeleton (Justus et al., 2004). However, to date, little attention has been paid to the relationship

between the UPP and the organization of the cytoskeleton in plants, particularly to the actin cytoskeleton, although the colocalization of proteasomes with actin and myosin has been reported in animal cells (Arcangeletti et al., 1997, 2000). Here, we report that inhibition of proteasome activity induces a time-dependent depolymerization of F-actin in pollen tubes. In addition, the MG132-induced inhibition of cytoplasmic streaming and loss of polarized distribution of organelles were observed in this study. These effects of MG132 are partially reminiscent of previous studies, which reported that the inhibition of actin polymerization in pollen tubes completely blocked tube growth and reduced organelle motility to Brownian motion, resulting in the appearance of ER in the extreme apices of tubes (Vidali et al., 2001; Justus et al., 2004). Moreover, inhibitor-induced disorganization of the MT cytoskeleton, especially in the swollen tip region, was also detected in this experiment, similar to a recent report that MG132 has effects on the organization of the MT cytoskeleton in synchronized tobacco (*Nicotiana tabacum*) cells (Oka, et al., 2004). All of these data are consistent with our theoretical prediction that inhibition of proteasome activity disorganized the cytoskeleton in pollen tubes.

The dynamic state of the cytoskeleton is controlled via numerous regulatory proteins (Vidali et al., 2001; Chen et al., 2002; Fu et al., 2002; Gu et al., 2003). Besides, the tip-focused Ca^{2+} is also involved in the cytoskeleton organization. Our data indicate that MG132 treatment did not cause an apparent disruption of calcium gradient in pollen tubes. Moreover, neither actin nor tubulin was ubiquitinated, and none of them accumulated in pollen tubes treated with MG132. Therefore, it is reasonable for us to speculate that the UPP might be involved in cytoskeleton dynamics mainly through a coordination of regulatory proteins essential for cytoskeleton organization, which was indeed observed in the earlier investigations. For example, Wang et al. (2003) revealed that RhoA, an important regulator for actin cytoskeleton dynamics, was temporally and spatially coordinated by the UPP. Besides, neural Wiskott-Aldrich syndrome protein, a protein regulating reorganization of the actin cytoskeleton through activation of the Arp2/3 complex, was degraded in a proteasome-dependent manner (Park et al., 2005). LIM kinase 1, a protein that controls many important cellular functions including growth cone actin dynamics, was also degraded by proteasome (Tursun et al., 2005). Furthermore, MT-associated protein τ (David et al., 2002; Zhang et al., 2005) and tubulin-folding cofactor B (Wang et al., 2005b) were proved to be degraded by 26S proteasome in animal cells. More recently, Aprea et al. (2006) found that MT-associated protein 2, a protein critical for MT nucleation, polymerization, stability, and bundling, was also degraded by proteasome. In short, our speculation that inhibition of proteasome disrupts the turnover of some short-lived regulatory proteins necessary for cytoskeleton dynamics is consistent with the conclusions mentioned above.

Cell wall extensibility is another key factor that regulates polarized tip growth in pollen tubes (Li et al., 1997, 2002; Parre and Geitmann, 2005). Our immunolabeling experiments with the JIM5 and JIM7 antibodies indicate that, in control tubes, acidic pectin is present in cell walls along the length of the tubes, except for the extreme apex. Esterified pectins are concentrated at the elongating tip, further confirming that pectins are secreted primarily as methylesters (Li et al., 1997, 2002) and are subsequently deesterified by pectin methylesterase in the cell wall (Micheli, 2001; Li et al., 2002). Calcofluor labeling revealed that cellulose is distributed throughout the tube walls, including the extreme apex, which is consistent with a previous report that cell walls at the tips of *P. abies* pollen tubes contain cellulose (Lazzaro et al., 2003). Moreover, the immunolabeling of pectins and calcofluor staining of cellulose presented in this study have revealed that inhibition of proteasome induces a marked decline in these cell wall components in pollen tubes, especially in the apical and subapical regions. This proteasome-inhibitor-induced decline in cell wall components was also further strengthened by FTIR analysis. Yet, we cannot explain the precise mechanism leading to this phenomenon. The most probable explanation is that MG132 disrupts the organization of the cytoskeleton, especially F-actin, inhibiting the transport of vesicles containing cell wall precursors such as esterified pectins (Li et al., 1997, 2002) and cellulose synthase (Moscatelli and Cresti, 2001). Interestingly, MG132 treatment prevents intracellular trafficking of PIN2 and gravibending of Arabidopsis (*Arabidopsis thaliana*) root apices (Abas et al., 2006). Alternatively, the inhibitor-induced disruption might affect the secretory system, especially the ER, resulting in the weakening of cell walls. Another possibility that cannot be excluded is that the inhibition of proteasome activity inhibits the turnover of enzymes associated with cell wall organization. In any case, the fact that MG132 treatment weakens tube walls is beyond doubt. Given that plant cell growth is driven by internal turgor pressure as well as propulsion force generated by the cytoskeletal elements (Baluška and Volkmann, 2002), and is restricted by the ability of the cell wall to extend under these forces (Parre and Geitmann, 2005), we conclude that inhibitor-induced cytoplasmic vacuolization and weakened cell wall are the most important factors in the formation of swollen tube tips and irregularly broadened tube diameters.

In summary, our investigations of the effects of MG132 on *P. wilsonii* pollen tubes have provided a more global view on the roles of the UPP in polarized tip growth in pollen tubes. It was revealed that inhibition of proteasome promoted accumulation of UbPs, which caused ER-derived cytoplasmic vacuolization and disruption of cytoskeleton in pollen tubes. Consequently, reduction of vesicle trafficking and the disorganization of cell wall led to the disruption of tip growth, which are summarized in Figure 13. This study provided two findings: (1) inhibition of proteasome

activity induces disruption of cytoskeleton in a time-dependent manner; and (2) inhibitor treatment causes a sharp decline in the main cell wall components of pollen tubes, such as cellulose and pectins, especially in the apical and subapical regions. The ER-derived cytoplasmic vacuolization occurring in gymnosperm pollen tubes in response to proteasome inhibitor treatment is also an interesting result. Taken together, our data revealed that the UPP is essential for maintaining the tip growth of *P. wilsonii* pollen tubes.

MATERIALS AND METHODS

Plant Material and in Vitro Pollen Culture

Mature pollen was collected from *Picea wilsonii* trees growing in the Botanical Garden of the Institute of Botany, Chinese Academy of Sciences, in April, 2004 and stored at −20°C until use. In vitro pollen culture was performed by liquid mass culture in an Erlenmeyer flask. The standard germination medium contained 12% (w/v) Suc, 0.01% (w/v) H_3BO_3, and 0.01% (w/v) $CaCl_2$, according to Hao et al. (2005) with some modifications. After 30 min of rehydration at room temperature under 100% relative humidity, pollen grains (1 mg mL^{-1}) were suspended in germination medium. Proteasome inhibitors MG132, Epoxomicin, and Cys-protease inhibitor E-64 were separately added into the culture medium from the initiation of culture at the concentrations indicated in the figure legends, or 40 μM MG132 was added into the culture medium when pollen grains had been cultured for 20 h in standard medium. For recovery experiments, pollen grains were treated with 40 μM MG132 for 20 h, then the inhibitor was removed, and tubes were reincubated in fresh complete medium without proteasome inhibitor. Controls were set up by adding the same amount of dimethylsulfoxide (Sigma) solvent for MG132. Solvent concentrations were never higher than 0.2%. All of the samples were cultured on a shaker (121 rpm) at 24°C in the dark. Unless otherwise stated, images of pollen tubes cultured in different media were randomly taken at the indicated time in the figure legends with an image analyzer-Q500 IW optical microscope (Zeiss). Germination rates and tube lengths were determined by scoring at least 300 randomly chosen pollen grains for each treatment. Pollen was considered germinated only when the tube length was greater than the diameter of the grain.

Proteasome Activity Assay

The proteasome activity was assayed according to Lightcap et al. (2000), with some modifications. In brief, pollen tubes cultured in standard medium for 24 h were collected and washed twice with phosphate-buffered saline (PBS) and then were ground to fine powder in a mortar with sand and liquid nitrogen. The resulting powder was resuspended in TNESV buffer (50 mM Tris-HCl, pH 7.5, 1% Nonidet P-40 detergent, 2 mM EDTA, 100 mM NaCl, and 10 mM sodium orthovanadates) without protease inhibitors. The supernatant obtained after a 15-min centrifugation at 500*g* was used for protein determination (Lowry et al., 1951) and proteasome activity assay. A total 200 μg of protein was used for kinetic measurement of proteasome chymotrypsin activity in the presence of 0.12 mM synthetic fluorogenic peptide chymotrypsin substrate sLLVY-AMC (Sigma). The MG132-induced inhibition of proteasome activity was validated by adding various concentrations of the inhibitor into the supernatant just prior to the proteasome assay. The breakdown of the peptide was monitored using a fluorescence spectrophotometer (F-4500, Hitachi) with an excitation wavelength of 370 nm and an emission wavelength of 430 nm. Primary experiments indicated that the signal was linear between 3 and 60 min. Thus, all samples were incubated at room temperature for 3 min and were then continuously monitored for 5 min.

Preparation of Protein Extracts and Immunoblotting Analysis

Method for immunoblotting analysis was according to Speranza et al. (2001) with some modification. Samples were collected and ground to fine powder in a mortar with sand and liquid nitrogen. This powder was resuspended in 50 mM Tris-HCl, pH 6.8, containing 1% (w/v) SDS, 5% (v/v) glycerol, and 2.5% (v/v) mercaptoethanol, and protease inhibitors such as 2 mM EGTA, 2 μg/mL aprotinin, and 1 μM phenylmethylsulfonyl fluoride. The suspensions were sonicated three times for 30 s, with a 30-s interval, and were then boiled for 10 min and centrifuged at 14,000*g* for 15 min. Fifty micrograms of protein from each sample were separated by SDS-PAGE on 12% polyacrylamide gels. Low molecular mass markers (14.4–97 kD; Amersham) were used as standards. The gels were then stained with Coomassie Blue or transferred onto nitrocellulose membranes (0.45-μm pores). The resulting blots were blocked with 3% bovine serum albumin (BSA)/PBS for 1 h at room temperature and probed overnight with antiubiquitin antibody (1:100; Sigma), or with an antiactin antibody (1:200; Sigma) or an anti-β-tubulin antibody (1:200; Sigma), and immune complexes were detected using horseradish peroxidase-conjugated secondary antibodies and 3,3′-diaminobenzidine.

TEM Observation

Samples (control and MG132-treated) were collected and fixed for 2 h at room temperature in 100 mM phosphate buffer, pH 7.2, containing 2.5% glutaraldehyde and 2% paraformaldehyde. After three washes in the same buffer for 30 min, samples were postfixed at 4°C overnight in phosphate buffer containing 1% osmium tetroxide, dehydrated in an ethyl-alcohol series, transferred to propylene oxide, embedded in Epon 812, and polymerized by heat. Ultrathin sections (70 nm thick) were obtained with a Leica ultramicrotome, stained with uranyl acetate and lead citrate, and observed under a JEM-1230 TEM (JEOL).

Immunogold Labeling Analysis of UbPs

For immunogold labeling of UbPs and free ubiquitin, samples were fixed for 1 h in ice-cold 0.1 M phosphate buffer, pH 7.2, containing 2.5% paraformaldehyde and 0.2% glutaraldehyde and then were embedded in LR White resin (Sigma) and polymerized by heat. Ultrathin sections were obtained and transferred to nickel grids that were then blocked with 3% BSA in PBS, pH 7.4, for 15 min and incubated overnight in a moist chamber with ubiquitin polyclonal antibody (Sigma) diluted 1:5 in 3% BSA/PBS. After three washes in 0.05 M Tris-HCl, pH 7.6, for 30 min, the sections were incubated for 2 h with a goat anti-rabbit IgG coupled to 10-nm gold particles (Sigma), diluted 1:50 in 0.5 M NaCl, buffered pH 8.0, containing 0.1% BSA, 0.05% Tween 20, and 5% fetal bovine serum. Finally, sections were rinsed in 0.05 M Tris-HCl and distilled water separately, stained with 2% uranyl acetate for 20 min, and observed under a JEM-1230 TEM (JEOL). All the sections were incubated simultaneously and using the same antibodies, except for the negative controls that were treated as described, but omitting the primary antibody. The quantity and distribution of UbPs in control and MG132-treated tubes were analyzed by the point-counting method (Rivett et al., 1992) on 30 different and randomly selected electron micrographs of each organelle (cytosol and ER), respectively.

Fluorescence Labeling of Cytoskeleton

Samples were fixed at room temperature in 50 mM PIPES buffer, pH 6.9, containing 4% paraformaldehyde for 1 h. For F-actin labeling, the pollen tubes were incubated in 1% Triton X-100/PBS for 1 h and then incubated in 1 μM phalloidin-FITC in PBS, pH 6.9, buffer for 2 to 3 h in the dark. The immunolabeling of MTs was performed according to Lazzaro (1999). Briefly, pollen tubes were permeabilized for 2 to 3 h in 1% Triton X-100/PBS after enzymatic digestion or freeze shattering. The resulting samples were then incubated with monoclonal antibody against β-tubulin (Sigma) and FITC-conjugated secondary antibody (Sigma). Control omitting primary antibody was also prepared. Thereafter, all the samples were washed, mounted on slides in 5% n-propyl gallate in glycerol, and observed under a Zeiss LSM 510 META laser-scanning confocal microscope, with an excitation wavelength of 488 nm and an emission wavelength of 522 nm.

Fluorescence Labeling of Ca^{2+}

Pollen tubes were cultured for 24 h and then loaded with the Ca^{2+}-sensitive fluorescent dye Fluo-3/AM ester (Sigma), which is highly lipophilic and thus easily crosses the plasma membrane by a nondisruptive route. Samples were incubated at 4°C in the dark in culture medium containing 20 μM Fluo-3/AM ester (prepared with dimethylsulfoxide) for 2 h. After this, the pollen tubes were rinsed three times with corresponding media and then cultured for additional 1 h.

Then the samples were excited with a 488-nm argon laser using the laser-scanning confocal microscope. Emission signals were collected at 515 nm.

Cytoplasmic Streaming Observation

To monitor cytoplasmic streaming, pollen tubes (both control tubes and MG132-treated tubes) were cultured for 24 h, then time-lapse images of pollen tube over 20 min (100 frames at about 12–14 s per frame) were captured, using a Zeiss confocal microscope equipped with CCD camera. Recovery experiments were also performed when tubes were treated with 40 μM MG132 for 20 h, then the inhibitor was removed. Subsequently, tubes were reincubated in fresh complete medium without proteasome inhibitor for 0.5 to 1 h.

Fluorescence Labeling of Pectin and Cellulose

Pollen tubes were fixed as described above. For immunolabeling of pectin, samples were blocked with 3% BSA/PBS for 30 min, which was followed by incubating samples with rat antiacidic pectin antibody (JIM5) or rat antiesterified pectin antibody (JIM7) at a dilution of 1:5 at room temperature for 2 h. After incubation, samples were rinsed in PBS three times (10 min each) and were incubated with a FITC-labeled sheep anti-rat IgG (Sigma), diluted 1:200 with PBS, pH 7.2, at room temperature for 45 min. After a final rinse series in PBS, the samples were mounted on slides and observed with the confocal laser-scanning microscope, as described above. For fluorescence labeling of cellulose, samples were washed and stained with 1 mg/mL calcofluor (Sigma), as described by Lazzaro et al. (2003), and then observed under a fluorescent microscope (Zeiss).

FTIR Analysis

FTIR analysis was according to Wang et al. (2005a) with some modification. Samples were collected after 24 h of incubation, washed with deionized water three times, and then dried on a barium fluoride window (13-mm diameter $\times$ 2 mm). Infrared spectra were obtained from the tip, subapical region, and base region of pollen tubes, respectively, with a MAGNA 750 FTIR spectrometer (Nicolet) equipped with a mercury-cadmium-telluride detector. The spectra were obtained at a resolution of 8 cm^{-1} with 128 coadded interferograms and were normalized to obtain the relative absorbance.

Statistics

Unless otherwise stated, all experiments were performed at least in triplicate. One-way ANOVA was used to compare the difference between the treated and control pollen tubes. Values of $P < 0.05$ were taken as statistically significant.

ACKNOWLEDGMENTS

We thank Drs. Richard Turner and Mathew Benson for their patient correction of the draft of the manuscript, and Dr. H.C. Zheng for his enlightening discussions.

Received April 7, 2006; revised June 6, 2006; accepted June 6, 2006; published June 15, 2006.

LITERATURE CITED

Abas L, Benjamins R, Malenica N, Paciorek T, Wisniewska J, Moulinier-Anzola JC, Sieberer T, Friml J, Luschnig C (2006) Intracellular trafficking and proteolysis of the Arabidopsis auxin-efflux facilitator PIN2 are involved in root gravitropism. Nat Cell Biol **8:** 249–256

Alché JD, Butowt R, Castro AJ, RodrÌguez-GarcÌa MI (2000) Ubiquitin and ubiquitin-conjugated proteins in the olive (*Olea europaea* L.) pollen. Sex Plant Reprod **12:** 285–291

Aprea S, Del Valle L, Mameli G, Sawaya BE, Khalili K, Peruzzi F (2006) Tubulin-mediated binding of human immunodeficiency virus-1 Tat to the cytoskeleton causes proteasomal-dependent degradation of microtubule-associated protein 2 and neuronal damage. J Neurosci **26:** 4054–4062

Arcangeletti C, de Conto F, Sutterlin R, Pinardi F, Missorini S, Geraud G, Aebi U, Chezzi C, Scherrer K (2000) Specific types of prosomes distribute differentially between intermediate and actin filaments in epithelial, fibroblastic and muscle cells. Eur J Cell Biol **79:** 423–437

Arcangeletti C, Sutterlin R, Aebi U, de Conto F, Missorini S, Chezzi C, Scherrer K (1997) Visualization of prosomes (MCP-proteasomes), intermediate filament and actin networks by ''instantaneous fixation'' preserving the cytoskeleton. J Struct Biol **119:** 35–58

Baluška F, Volkmann D (2002) Actin-driven polar growth of plant cells. Trends Cell Biol **12:** 14

Chen CY, Wong EI, Vidali L, Estavillo A, Hapler PK, Wu HM, Cheung AY (2002) The regulation of actin organization by actin-depolymerizing factor in elongating pollen tubes. Plant Cell **14:** 2175–2190

Ciechanover A (2005) Intracellular protein degradation: from a vague idea thru the lysosome and the ubiquitin-proteasome system and onto human diseases and drug targeting. Cell Death Differ **12:** 1178–1190

David DC, Layfield R, Serpell L, Narain Y, Goedert M, Spillantini MG (2002) Proteasomal degradation of tau protein. J Neurochem **83:** 176–185

Franklin-Tong VE (1999) Signaling and the modulation of pollen tube growth. Plant Cell **11:** 727–738

Fribley A, Zeng Q, Wang CY (2004) Proteasome inhibitor PS-341 induces apoptosis through induction of endoplasmic reticulum stress-reactive oxygen species in head and neck squamous cell carcinoma cells. Mol Cell Biol **24:** 9695–9704

Fu Y, Li H, Yang Z (2002) The ROP2 GTPase controls the formation of cortical fine F-actin and the early phase of directional cell expansion during Arabidopsis organogenesis. Plant Cell **14:** 777–794

Glickman MH, Ciechanover A (2002) The ubiquitin-proteasome proteolytic pathway: destruction for the sake of construction. Physiol Rev **82:** 373–428

Gu Y, Vernoud V, Fu Y, Yang Z (2003) ROP GTPase regulation of pollen tube growth through the dynamics of tip-localized F-actin. J Exp Bot **54:** 93–101

Hampton RY (2002) ER-associated degradation in protein quality control and cellular regulation. Curr Opin Cell Biol **14:** 476–482

Hao HQ, Li YQ, Hu YX, Lin JX (2005) Inhibition of RNA and protein synthesis in pollen tube development of *Pinus bungeana* by actinomycin D and cycloheximide. New Phytol **165:** 721–730

Hellmann H, Estelle M (2002) Plant development: regulation by protein degradation. Science **297:** 793–797

Hershko A (2005) The ubiquitin system for protein degradation and some of its roles in the control of the cell division cycle. Cell Death Differ **12:** 1191–1197

Hiller MM, Finger A, Schweiger M, Wolf DH (1996) ER degradation of a misfolded luminal protein by the cytosolic ubiquitin-proteasome pathway. Science **273:** 1725–1728

Justus CD, Anderhag P, Goins JL, Lazzaro MD (2004) Microtubules and microfilaments coordinate to direct a fountain streaming pattern in elongating conifer pollen tube tips. Planta **219:** 103–109

Kulikauskas R, Hou A, Muschietti J, McCormick S (1995) Comparisons of diverse plant species reveal that only grasses show drastically reduced levels of ubiquitin monomer in mature pollen. Sex Plant Reprod **8:** 326–332

Lazzaro MD (1999) Microtubule organization in germinated pollen of the conifer *Picea abies* (Norway spruce, Pinceae). Am J Bot **86:** 759–766

Lazzaro MD, Donohue JM, Soodavar FM (2003) Disruption of cellulose synthesis by isoxaben causes tip swelling and disorganizes cortical microtubules in elongating conifer pollen tubes. Protoplasma **220:** 201–207

Lee DH, Goldberg AL (1998) Proteasome inhibitors: valuable new tools for cell biologists. Trends Cell Biol **8:** 397–403

Li Y, Zee SY, Liu YM, Huang BQ, Yen LF (2001) Circular F-actin bundles and a G-actin gradient in pollen and pollen tubes of *Lilium davidii*. Planta **213:** 722–730

Li YQ, Mareck A, Faleri C, Moscatelli A, Liu Q, Cresti M (2002) Detection and localization of pectin methylesterase isoforms in pollen tubes of *Nicotiana tabacum* L. Planta **214:** 734–740

Li YQ, Moscatelli A, Cai G, Cresti M (1997) Functional interactions among cytoskeleton, membranes and cell wall in pollen tubes of flowering plants. Int Rev Cytol **176:** 133–199

Lightcap ES, McCormack TA, Pien CS, Chau V, Adams J, Elliott PJ (2000) Proteasome inhibition measurements: clinical application. Clin Chem **46:** 673–683

Lowry OH, Rosebrough NJ, Farr AL, Randall RJ (1951) Protein measurement with the Folin phenol reagent. J Biol Chem **193:** 265–275

Mascarenhas JP (1993) Molecular mechanisms of pollen tube growth and differentiation. Plant Cell **5:** 1303–1314

McCann MC, Hammouri M, Wilson R, Belton P, Roberts K (1992) Fourier transform infrared microspectroscopy is a new way to look at plant cell walls. Plant Physiol **100:** 1940–1947

McCann MC, Shi J, Roberts K, Carpita NC (1994) Changes in pectin structure and localization during the growth of unadapted and NaCl-adapted tobacco cells. Plant J **5:** 773–785

Micheli F (2001) Pectin methylesterases: cell wall enzymes with important roles in plant physiology. Trends Plant Sci **6:** 414–419

Mimnaugh EG, Xu W, Vos M, Yuan X, Isaacs JS, Bisht KS, Gius D, Neckers L (2004) Simultaneous inhibition of hsp 90 and the proteasome promotes protein ubiquitination, causes endoplasmic reticulum-derived cytosolic vacuolization, and enhances antitumor activity. Mol Cancer Ther **3:** 551–566

Moscatelli A, Cresti M (2001) Pollen germination and pollen tube growth. *In* SS Bhoiwani, WY Soh, eds, Current Trends in the Embryology of Angiosperms. Kluwer Academic Publishers, Dordrecht, The Netherlands, pp 33–65

Oka M, Yanagawa Y, Asada T, Yoneda A, Hasezawa S, Sato T, Nakagawa H (2004) Inhibition of proteasome by MG-132 treatment causes extra phragmoplast formation and cortical microtubule disorganization during M/G1 transition in synchronized tobacco cells. Plant Cell Physiol **45:** 1623–1632

Park SJ, Suetsugu S, Takenawa T (2005) Interaction of HSP90 to N-WASP leads to activation and protection from proteasome-dependent degradation. EMBO J **24:** 1557–1570

Parre E, Geitmann A (2005) Pectin and the role of the physical properties of the cell wall in pollen tube growth of *Solanum chacoense.* Planta **220:** 582–592

Qiao H, Wang HY, Zhao L, Zhou JL, Huang J, Zhang YS, Xue YB (2004) The F-box protein AhSLF-S-2 physically interacts with S-RNases that may be inhibited by the ubiquitin/26S proteasome pathway of protein degradation during compatible pollination in antirrhinum. Plant Cell **16:** 582–595

Rabinovich E, Kerem A, Frohlich KU, Diamant N, Bar-Nun S (2002) AAA-ATPase p97/Cdc48p, a cytosolic chaperone required for endoplasmic reticulum-associated protein degradation. Mol Cell Biol **22:** 626–634

Rivett AJ, Palmer A, Knecht E (1992) Electron microscopic localization of the multicatalytic proteinase complex in rat liver and in cultured cells. J Histochem Cytochem **40:** 1165–1172

Scoccianti V, Ovidi E, Taddei AR, Tiezzi A, Crinelli R, Gentilini L, Speranza A (2003) Involvement of the ubiquitin/proteasome pathway in the organisation and polarised growth of kiwifruit pollen tubes. Sex Plant Reprod **16:** 123–133

Sheng XY, Hu ZH (2005) Effects of MG132, an inhibitor of proteasome, on the pollen germination and tube growth of *Picea wilsonii.* Shi Yan Sheng Wu Xue Bao **38:** 309–316

Speranza A, Scoccianti V, Crinelli R, Calzoni GL, Magnani M (2001) Inhibition of proteasome activity strongly affects kiwifruit pollen germination: involvement of the ubiquitin/proteasome pathway as a major regulator. Plant Physiol **126:** 1150–1161

Taylor LP, Hepler PK (1997) Pollen germination and tube growth. Annu Rev Plant Physiol Plant Mol Biol **48:** 461–491

Tursun B, Schluter A, Peters MA, Viehweger B, Ostendorff HP, Soosairajah J, Drung A, Bossenz M, Johnsen SA, Schweizer M, et al (2005) The ubiquitin ligase Rnf6 regulates local LIM kinase 1 levels in axonal growth cones. Genes Dev **19:** 2307–2319

Varshavsky A (2005) Regulated protein degradation. Trends Biochem Sci **30:** 283–286

Vidali L, Hepler PK (2001) Actin and pollen tube growth. Protoplasma **215:** 64–76

Vidali L, McKenna ST, Hepler PK (2001) Actin polymerization is essential for pollen tube growth. Mol Biol Cell **12:** 2534–2545

Vitale A, Denecke J (1999) The endoplasmic reticulum-gateway of the secretory pathway. Plant Cell **11:** 615–628

Wagenknecht B, Hermisson M, Groscurth P, Liston P, Krammer PH, Weller M (2000) Proteasome inhibitor-induced apoptosis of glioma cells involves the processing of multiple caspases and cytochrome c release. J Neurochem **75:** 2288–2297

Wang HR, Zhang Y, Ozdamar B, Ogunjimi AA, Alexandrova E, Thomsen GH, Wrana JL (2003) Regulation of cell polarity and protrusion formation by targeting RhoA for degradation. Science **302:** 1775–1779

Wang QL, Kong L, Hao H, Xiaohua Wang X, Lin JX, Šamaj J, Baluška F (2005a) Effects of Brefeldin A on pollen germination and tube growth: antagonistic affects on endocytosis and secretion. Plant Physiol **139:** 1692–1703

Wang W, Ding J, Allen E, Zhu P, Zhang L, Vogel H, Yang Y (2005b) Gigaxonin interacts with tubulin folding cofactor B and controls its degradation through the ubiquitin-proteasome pathway. Curr Biol **15:** 2050–2055

Werner ED, Brodsky JL, McCracken AA (1996) Proteasome-dependent endoplasmic reticulum-associated protein degradation: an unconventional route to a familiar fate. Proc Natl Acad Sci USA **93:** 13797–13801

Zhang JY, Liu SJ, Li HL, Wang JZ (2005) Microtubule-associated protein tau is a substrate of ATP/Mg^{2+}-dependent proteasome protease system. J Neural Transm **112:** 547–555